Proceedings of Meetings on Acoustics

Volume 4, 2008 http://asa.aip.org

155th Meeting
Acoustical Society of America
Paris, France
29 June - 4 July 2008
Session 5aUWb: Underwater Acoustics

5aUWb1. Spatial and Temporal Variations in Acoustic propagation during the PLUSNet'07 Exercise in Dabob Bay

Jinshan Xu, Pierre F. Lermusiaux, Patrick J. Haley Jr., Wayne G. Leslie and Oleg G. Logutov

We present the spatial and temporal variability of the acoustic field in Dabob Bay during the PLUSNet07 Exercise. The study uses a 4-D data-assimilative numerical ocean model to provide input to an acoustic propagation model. The ocean physics models (primitive-equations and tidal models), with CTD data assimilation, provided ocean predictions in the region. The output ocean forecasts had a 300m and 1-5m resolution in the horizontal and vertical directions, at 3-hour time intervals within a 15-day period. This environmental data, as the input to acoustic modeling, allowed for the prediction and study of the temporal variations of the acoustic field, as well as the varying spatial structures of the field. Using a one-way coupled-normal-mode code, along- and across-sections in the Dabob Bay acoustic field structures at 100, 400, and 900 Hz were forecasted and described twice-daily, for various source depths. Interesting propagation effects, such as acoustic fluctuations with respect to the source depth and frequency as a result of the regional ocean variability, wind forcing, and tidal effects are discussed. The novelty of this work lies in the possibility of accurate acoustic TL prediction in the littoral region by physically coupling the real-time ocean prediction system to real-time acoustic modeling.

Published by the Acoustical Society of America through the American Institute of Physics

 [DOI: 10.1121/1.2988093]
Received 9 Jul 2008; published 3 Sep 2008

Spatial and Temporal Variations in Acoustic propagation during the PLUSNet'07 Exercise in Dabob Bay[1]

Jinshan Xu, Pierre F.J. Lermusiaux , Patrick J. Haley Jr. , Wayne G. Leslie and Oleg G. Logutov

Massachusetts Institute of Technology, Department of Mechanical Engineering, 77 Massachusetts Avenue, Cambridge MA 02319, USA.

1. INTRODUCTION

Acoustic propagation in shallow water is a challenging scientific and engineering research topic and an area of major concern to the US Navy. Of particular interest is the influence of water column variability on acoustic propagation [1, 2] and communications [3]. In the recent Persistent Littoral Undersea Surveillance Network (PLUSNet) PN07 exercise in Dabob Bay, acoustic models, combined with the 4-D (3-D in space, 1-D in time) MIT numerical ocean models with data assimilation (MSEAS, including the Harvard Ocean Prediction System - HOPS) and seabed geoacoustic models were used to generate acoustic transmission loss (TL) reports on a daily basis. The joint ocean and acoustic predictions allowed for the investigation of acoustic TL and phase fluctuations due to the regional ocean variation, wind forcing, (internal) tide effects for different source depths and frequencies. A computational novelty of this research is the real-time combination of the ocean prediction system, acoustic modeling and data assimilation [4, 5, 6] in an internal bay of a fjord environment, the Hood Canal in Washington state.

2. THE INTEGRATION OF OCEAN AND ACOUSTIC MODELING

2.1. Ocean modeling

Physical processes and variabilities occur in the ocean on millimeters to planetary space scales and on seconds to climate time scales; all of which may significantly affect acoustic propagation. It has been noted that spatial variability of the sound speed field will introduce difficulties in range-dependent acoustic propagation modeling. MSEAS with HOPS [7], ESSE [8, 9] and tidal modeling [10] provides the opportunities to research these problems. The ocean sound speed prediction was provided on a daily basis during the PN07 exercise at 3-hour time interval.

To obtain accurate acoustic propagation modeling, the background sound speed profile is one of the most important factors. The acoustic modeling in this study is largely based on HOPS predictions to provide water column sound speed profiles. The geoacoustic model is provided by Naval Oceanographic Office (NAVOCEANO).

During the exercise, several research vessel and platforms conducted CTD measurements at various locations, depths, and times. An essential check of the validity of an ocean prediction system is to compare predictions to CTD measurements.

2.1.1. Sound speed profile variations

The PN07 experiment in Dabob Bay was an integrated experiment involving several different kinds of platforms, which included three surface research vessels (R/V Point Sur, R/V New Horizon, and R/V Wecoma), several Autonomous Underwater Vehicles (AUV) and Kayaks, and seven sea gliders. Figure 1 depicts all CTD sampling locations

[1] Corresponding authors: Pierre F.J. Lermusiaux (pierrel@mit.edu), Jinshan Xu (jinshan@mit.edu)

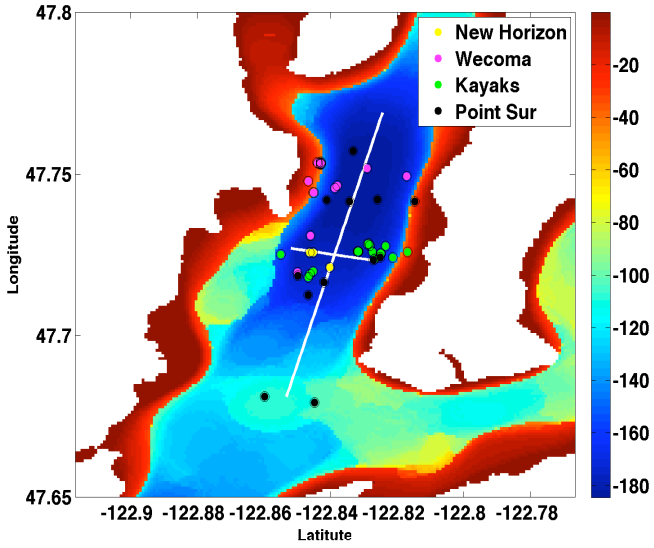

FIGURE 1. The bathymetry of Dabob Bay and CTD samplings' locations. The different color dots indicate the different platforms where the the CTD samplings were conducted .

during PN07 in Dabob Bay (except data from the SeaGliders). The different color dots indicate the different platforms where the CTD samplings were conducted . Four different platforms are listed: the three R/Vs and Kayaks.

The measured CTD profiles from each platform are shown in Figure 2. In each panel, there are two thick dark dashed lines (red and black) in addition to other solid thin lines. The solid thin lines are the sampling from that platform. The black dark dashed line is the average of the sound speed profiles from that single platform. The red dark dashed line is the average of the all sound speed profiles.

The interesting finding from those sound speed profiles is the persistent sound channel at a depth of 20 m during the PN07 experiment period. From the 50 m to 120 m depths there is an essentially constant sound speed background layer. In the center of Dabob Bay, the deep region from 120 m to the bottom, there is another low sound speed region that attracts sound energy. However, since it is close to the bottom, most energy will be either reflected, absorbed or attenuated by the bottom layer. Therefore, the sound channel at the near-surface depth of 20 m is the dominant sound channel for acoustic transmissions in the Dabob Bay. It can lead to significant sound attenuation, especially in "summer effect" conditions when the sea surface is heated and with characteristics of "quiet, near glass-like". The reported "perplexing result of seemingly poor acoustic propagation conditions" during the exercise on Oct. 10th was possibly a result of this effect. An illuminating example for the sound propagation is shown in Figure 3. As shown, the sound energy is mainly trapped in that sound channel at depth of 20 m for the frequency of 900 Hz.

To evaluate the MSEAS-HOPS output, we first compared CTD data to predicted sound speed across-bay sections, averaged over a day. In Figure 4, we show one example of these comparisons on Oct. 4th during the experiment. The left panel shows the bathymetry map of Dabob Bay and the CTD samples locations with different colors indicating the different platforms. The right top two panels show the sound speed section along/across Dabob Bay from the output of HOPS. The right bottom panels show the average sound speed profiles from HOPS and the CTD samplings from different platforms, respectively. In general, the HOPS prediction captured the most prominent character of 20 m depth sound channel and near bottom sound channel, but it lacks some details when compared to CTD samplings. This is in part due to the averaging and to the limited ocean data in the region.

2.2. Acoustic modeling

The normal modes code used here is called the Coupled SACLANTCEN normal mode propagation loss model (C-SNAP)[11]. It was developed as a range-dependent propagation loss model by Ferla, *et al*. on the base of a widely used

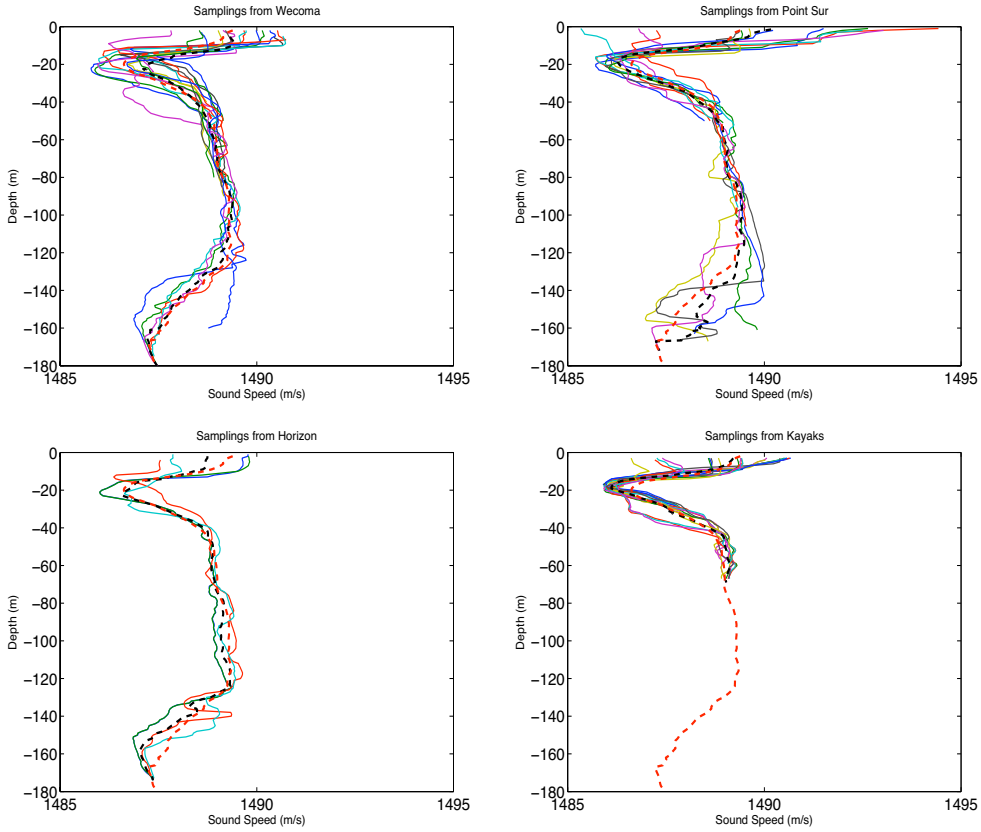

FIGURE 2. Sound speed profiles from different platforms. In each panel, there are two thick dark dashed lines (red and black) in addition to other solid thin lines. The thin lines are the sampling from that platform. The black dark dashed line is the average of the sound speed profiles from that single platform. The red dark dashed line is the average of the all sound speed profiles.

and efficient range-independent normal mode code, SNAP, and a numerical solution technique for one-wave mode coupling obtained from KRAKEN. Despite the great achievements obtained with fast field and parabolic equation models, normal mode programs still remain a very efficient, simple, and practical tool for describing ocean acoustics in range-independent environments. C-SNAP generalizes the range-independent problem to a range-dependent one by dividing the propagation path in a sequence of range-independent segments and using normal modes to represent the acoustic field in each segment. It uses a finite-difference algorithm to solve for the range-independent problem and assumes that the acoustic field is dominated by the outgoing component. To preserve accuracy, an energy-conserving matching condition is implemented at the coupling interfaces.

3. THE VARIATION OF ACOUSTIC TRANSMISSION LOSS IN DABOB BAY

3.1. Acoustic transmission loss with different geoacoustic models

Accurate acoustic propagation modeling requires knowledge of the bathymetry as well as the sediment geoacoustic properties. In addition to bathymetric data, NAVOCEANO generously provided sediment data in the form of HFEVA sediment types for Dabob Bay. The sediment types were translated into grain size and gridded. Sediment thickness varies greatly throughout Dabob Bay due to its complicated geologic history. However, Helton's 1976 report [12] on the Dabob Bay Range notes that the unconsolidated sediment varies to at least 4.5 feet (1.37 m). Lacking seismic reflection or similar ground-truth data, this value was adopted as a uniform sediment thickness in one of our geoacoustic models.

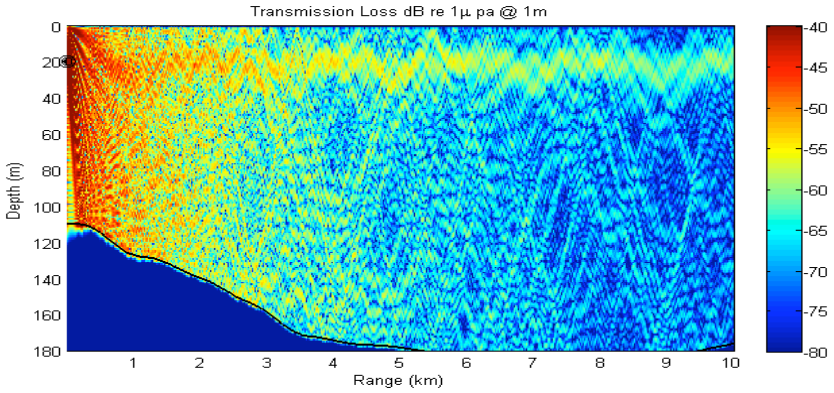

FIGURE 3. Acoustic Transmission Loss modeling for sound source with frequency 900 Hz and at depth of 20 m.

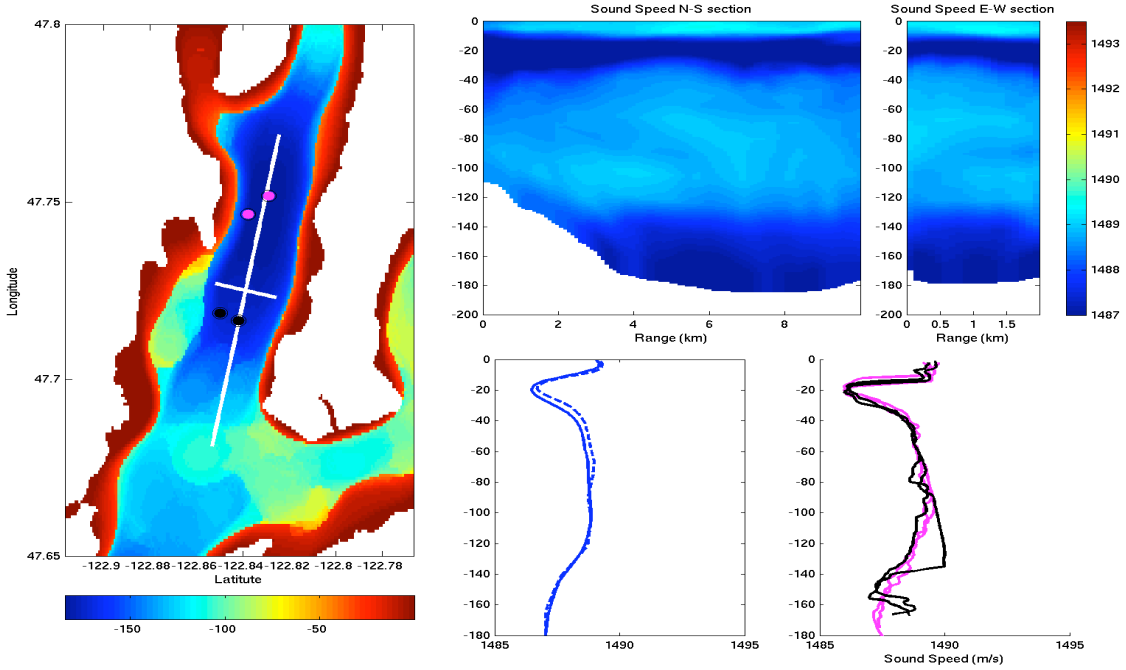

FIGURE 4. Comparison of sound speed profiles between the CTD data and HOPS output on Oct. 4th. The left panel shows the bathymetry map of Dabob Bay and the CTD samples locations with different colors indicating the different platforms. The right top two panels show the sound speed section along/across Dabob Bay from the output of HOPS. The right bottom panels show the average sound speed profiles from HOPS (solid blue line indicates the average of the sound speed file in the along Dabob section; the dashed blue line indicates the average of the sound speed file in the across Dabob section.) and the CTD samplings from different platforms respectively with different color indicate the location spotted in the left panel.

For the bottom layer, a grain size of 0 phi was chosen based upon Helton's report about: "...whatever the state of the surface sediment veneer (loose, hard, or dense/compacted), a harder underlaying layer most generally begins 3 to 50 feet below the mudline (contact with water) and consists of glacial till". Till is associated with moraines which has a sound speed ratio of 1.3 [13] . Similarly, the HFEVA "Muddy Sandy Gravel "sediment classification has a sound speed ratio of 1.2778 and a grain size of 0.

Two geoacoustic models were tested during PN07. The first was an isotropic 2-meter deep silt-clay sedimental layer

TABLE 1. Seabed properties of two geoacoustic models

	Silt-Clay Model	HFEVA Model	unit
Sediment Depth	2	1.3716	m
Sediment Density	1.376	1.7922	g/cm^3
Sediment Attenuation	0.6	0.128	dB/λ
Sediment Sound Speed	1522	1509	m/s
Bottom Density	2.5	2.08	g/cm^3
Bottom Attenuation	0.1	0.37	dB/λ
Bottom Sound Speed	2000	1764	m/s

on the hard bottom. This model was a rough estimate based on historical data and was used to test coupled acoustic-ocean predictions. Then, beginning with the first day of sea exercises, the second geoacoustic model, the HFEVA model, was suggested [14] as being closer to the real seabed bottom. This was then used for all subsequent studies. The main parameters of these two geoacoustic models are listed in Table 1. We note that both of our bottom models are overly simplistic for frequencies below 1 kHz. In reality, the subbottom sedimentation should be included in the geoacoustic model for our “low" frequencies.

Figure 5 shows an example for the frequency of 900 Hz, at source depth of 40 m. The lower panel shows the comparison of acoustic TL at the receiver depth of 8.4 m. These comparisons show the critical sensitivity of acoustical TL to the seabed bottom properties. The acoustic transmission loss calculations based on these two geoacoustic models are performed by CSNAP. The TL prediction is based on the narrow band model with frequency range from 100 Hz to 900 Hz, at varied depth of 20 m, 30 m, and 40 m.

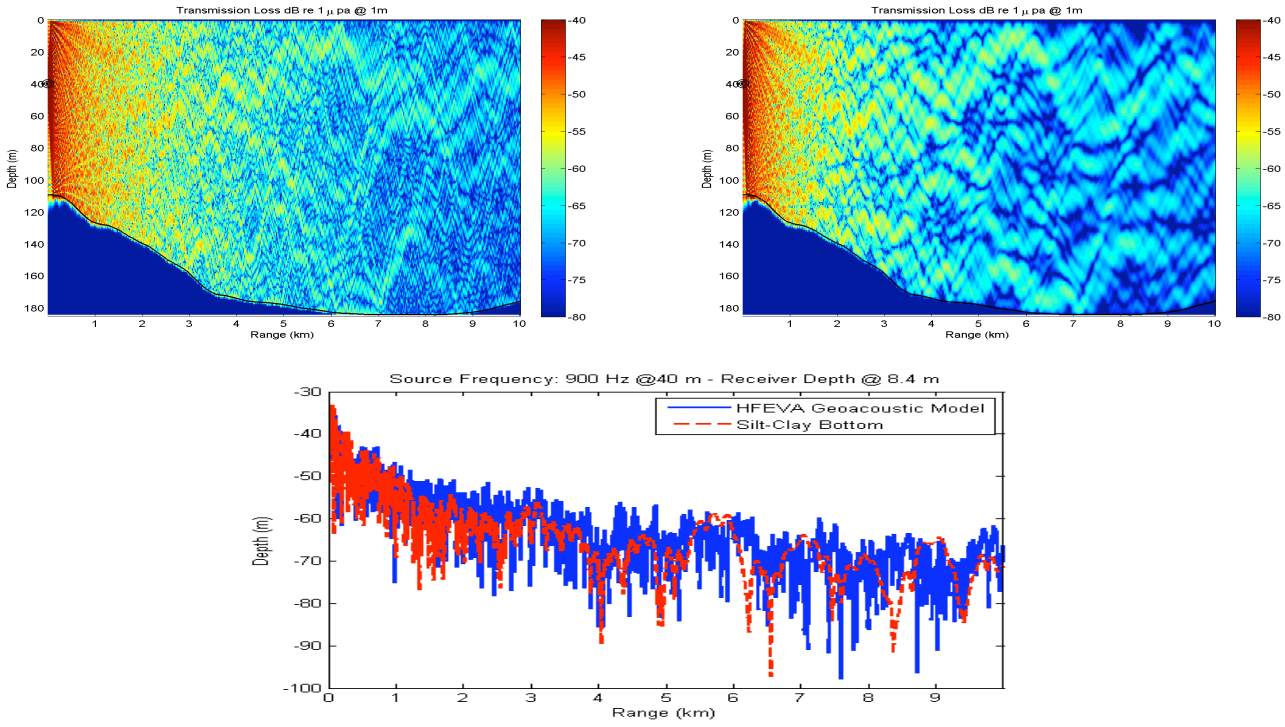

FIGURE 5. Acoustic TL prediction for 900 Hz source at depth of 40 m, for two different seabed geo-acoustic model. The upper left panel is silt-clay model; the upper right panel corresponds to the HFEVA model. The lower panel is the comparison of acoustic TL at the receiver depth of 8.4 m for these two geo-acoustic models.

3.2. Acoustic transmission loss variation over 7 days of the experiment and atmospheric forcing effects

The ocean sound speed section is obtained from HOPS output of temperature, salinity, and pressure. The sections along Dabob Bay with sound speed are shown in Figure 6. These are displays for 6 continuous days, from October 5th to October 10th, with one example for each day. The prominent characteristic is the warm surface layer in the first four days. In the fourth day (left lower panel), this warm surface layer started to disappear due to the wind forcing. In the acoustic point of view, it leads to more refraction than surface reflection.

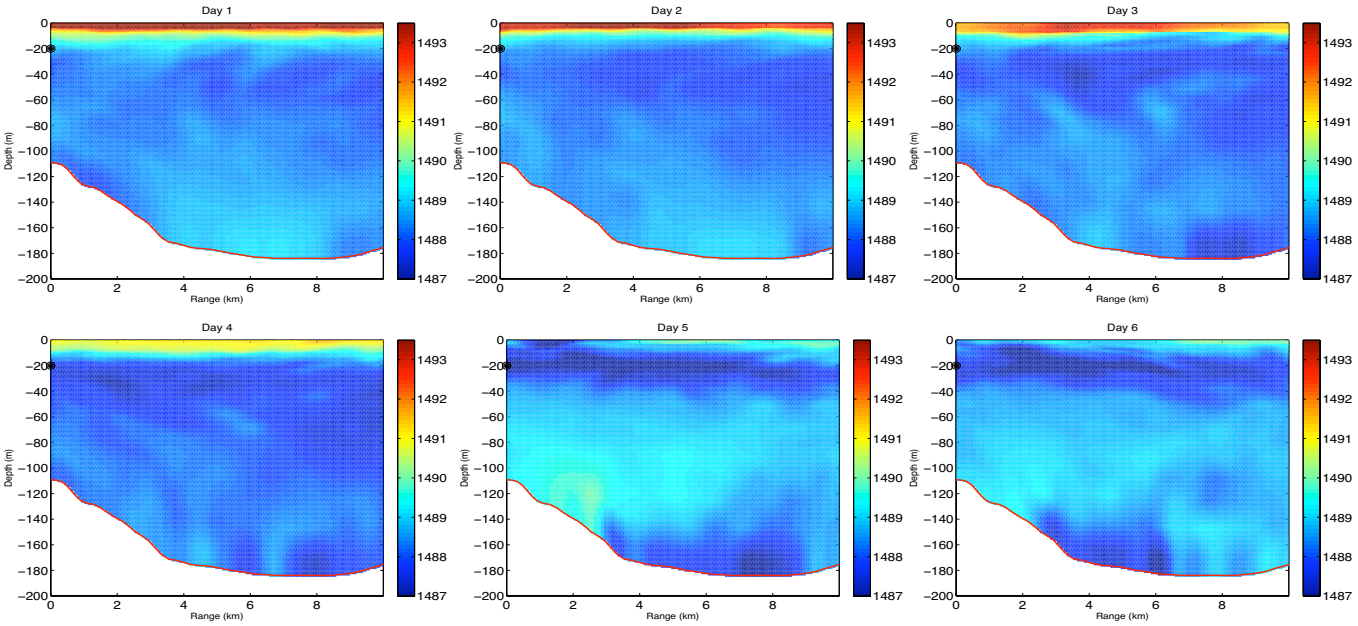

FIGURE 6. Sound speed fluctuation for six continuous days from the along Dabob Bay section. From left to right, and top to bottom, these six panels correspond to the days October 5 to 10, 2007.

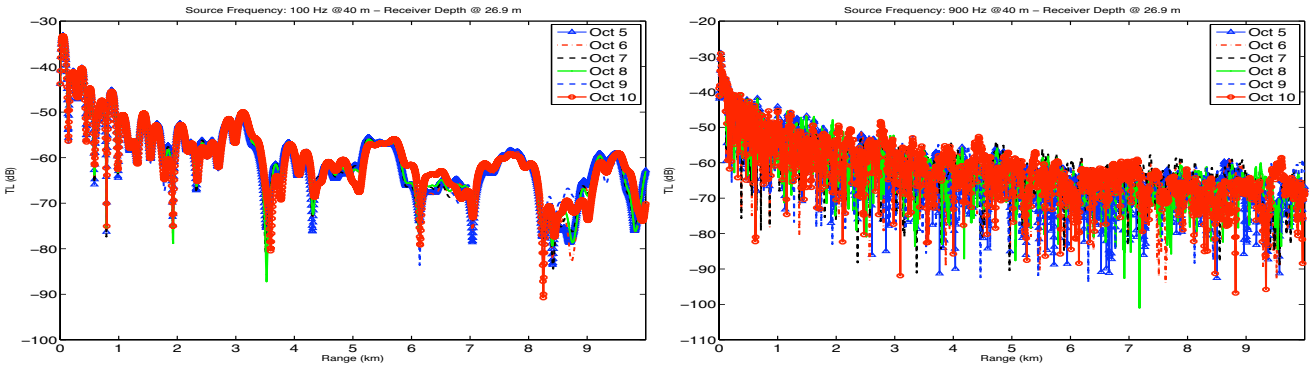

FIGURE 7. The comparisons of acoustic TL prediction along Dabob Bay of six continuous days (October 5 to 10, 2007) for frequency of 100 Hz source depth of 40 m (left), and 900 Hz at source depth of 40 m (right); receiver depth of 27 m.

The corresponding acoustic TL was calculated for different frequencies and source locations. Examples for the frequency of 100 Hz and 900 Hz at source depth of 40 m and receiver depth of 27 m are shown in Figure 7. We found that the lower frequency sound source (100 Hz) is less sensitive to the wind forcing (Figure 6) than the higher frequency sound source (900 Hz). There was strong wind forcing during the fourth and fifth days, which mixed the warm surface layer in the following days. For the lower frequency sound source, the variation of acoustic TL is not very sensitive to the upper boundary layer. We chose one particular receiver depth for the comparison of TL. The left

panel shows transmission loss of sound source with frequency of 100 Hz, the right panel shows transmission loss of sound source with frequency of 900 Hz for six continuous days. The discrepancies among different days for 900 Hz case are much more prominent than the 100 Hz case. There is about 10 dB dynamic range more in 900 Hz case than 100 Hz case.

3.3. Acoustic transmission loss variation due to tidal effects

To examine tidal effects on acoustic transmission loss, we utilized the MSEAS ocean environmental outputs at 3-hour intervals over a 12 hour period for the day of October 12th, as shown in the four panels of Fig. 8 which are along Dabob Bay sections.

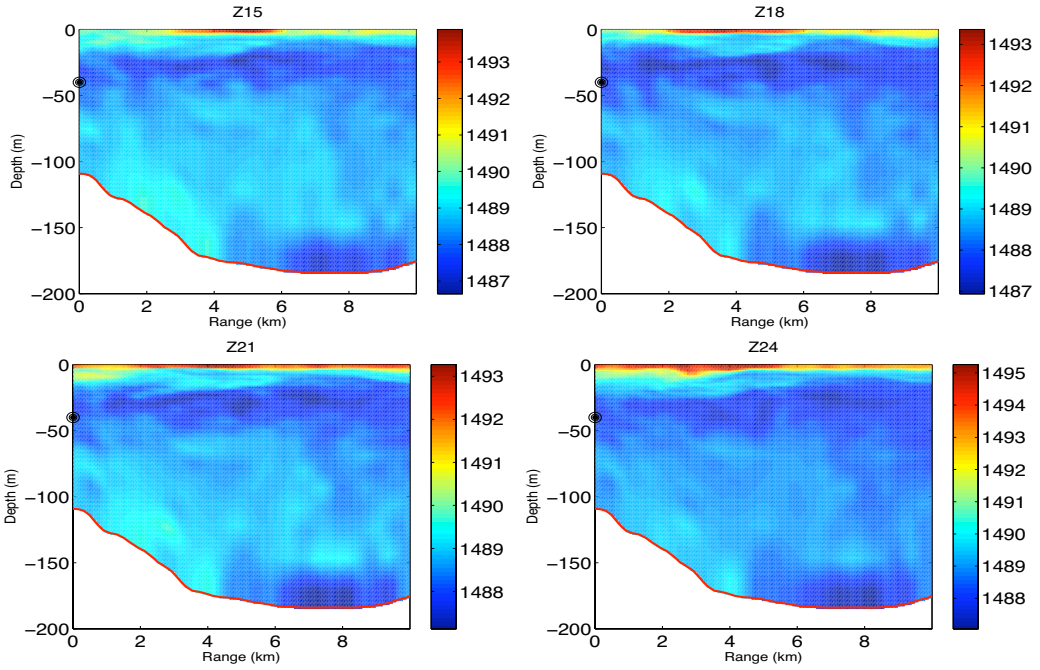

FIGURE 8. Sound speed fluctuation due to the tide effect in 12 hours period on Oct. 12th.

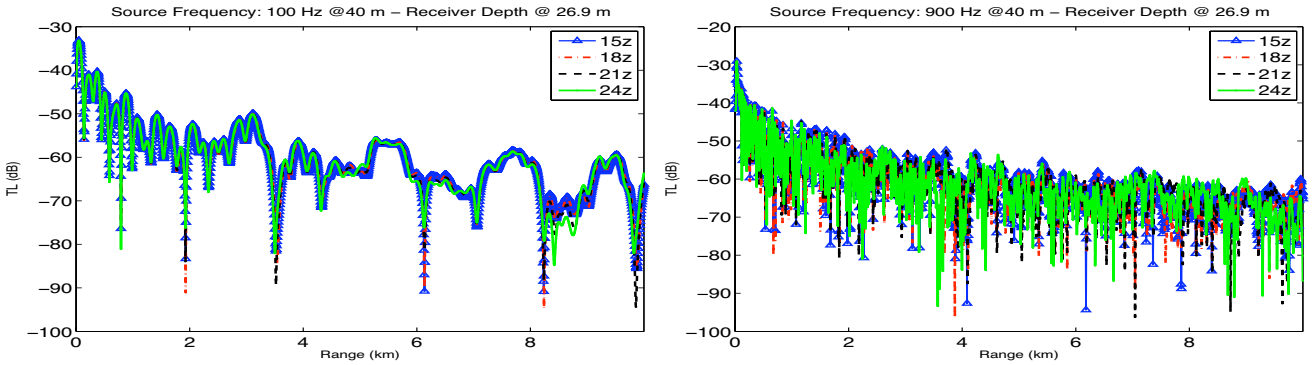

FIGURE 9. Acoustic TL prediction in the along Dabob Bay section for 100 and 900 Hz source at depth of 40 m, and receiver depth of 27 m. Four different color lines in the each panel indicate the TL prediction in one section at four different times during one tidal period.

The acoustic transmission loss for these four different sections with 3-hour interval over one tidal period is calculated for different frequencies and source depths. Here, we show the 100 Hz and 900 Hz cases, with sound source depths at

40 m and receiver depth at 27 m (see Figure 9). Note that these two panels have exactly the same configurations as the two panels showed in Figure 7, i.e. with source depth 40 m, receiver depth at 27 m.

Unlike the wind forcing effect, tidal effects did not significantly affect the acoustic TL prediction for the higher frequency source (900 Hz, right panel of Figure 9) in spatial scale. However, for the lower frequency sound source (100 Hz, left panel of Figure 9), tidal effects seem to perturb the sound energy more in some fixed distance, such as the null points at distance of 2, 3.5, 6, and 8 km. There are as much as 20 dB variations at those points in different time sections, while in Figure 7, there are only at most 10 dB variations at those null points on different days.

3.4. Frequency spectra of sound speed and acoustic variables

The study of acoustic propagation in shallow water has to cope with the spatially and temporally varying environmental field. An useful output of the acoustic calculation is a statistical representation of the field variability, such as the TL spectra density as a function of time for given geographical regions and seasons.

Based on the output (temperature, salinity, and pressure) of 4-D ocean water column fields of Dabob Bay with 3-hour time intervals and 15-day duration, the frequency spectra of sound speed fluctuation is estimated for certain ranges and depths. The average is taken among all the spectra estimations, which is shown in Figure 10. The spectral peaks are associated with diurnal and semidiurnal tide and the higher order tidal harmonics. The frequency spectra of acoustic variables (intensity and phase) are shown in Figure 11 for different source frequencies (corresponding different rows: 100, 400, and 900 Hz from top to bottom) and depths (corresponding to different columns: 20 m and 40 m from left to right). We find that tidal effects have much larger signatures in lower frequency and deeper source depth than higher frequency and shallower source depth.

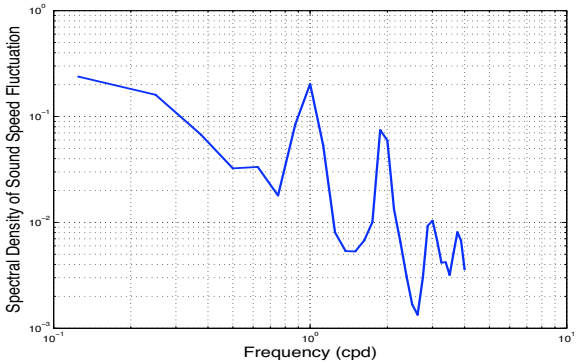

FIGURE 10. The frequency spectra density of sound speed fluctuation in Dabob Bay.

4. CONCLUSION

The integrated study, based on our MIT-MSEAS ocean prediction and data assimilation and on CSNAP acoustics propagation, shows the possibility of providing real-time acoustic transmission loss in shallow water environments, which is critical to the US Navy sub-sea exercises. In this study, we found that the seabed geoacoustic model has a strong influence on the the acoustic propagation prediction. The coupling allows implementing range-dependent acoustic propagation modeling based on the spatial variations of the speed of sound provided by MIT-MSEAS. During the exercise, we provided such predictions in two sections (across/along) of Dabob Bay. Here, we only discussed the along-bay section.

We studied acoustic fluctuations due to wind forcing and to tidal effects. The wind forcing disturbed the surface layer and affected the acoustic transmission, with different responses for different frequencies. For the low frequency (100 Hz), the wind forcing induced TL fluctuations (10 dB) in the section; for the high frequency (900 Hz), the TL fluctuations could reach to 20 dB in some distances. In fact, during the experiment, there were periods during which no acoustic signal could be received. An explanation is that the warm surface layer generated a perfect refraction mirror on the surface, concentrating the sound energy in specific paths. Once strong wind forcing started, the refraction layer was thickened, leading to higher sound energy scattering.

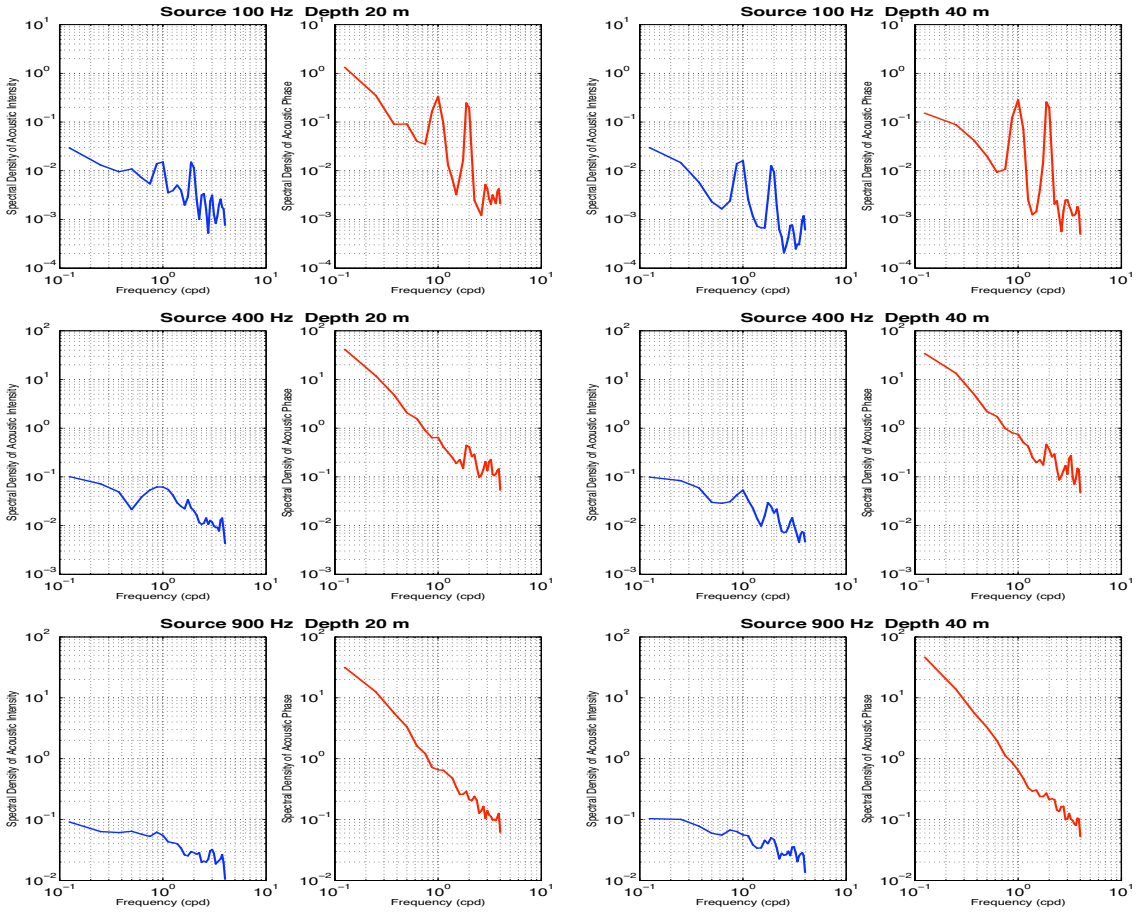

FIGURE 11. The frequency spectra density of acoustic variables (intensity - blue line and phase - red line) in Dabob Bay.

Tidal effects induce much bigger TL fluctuation (20 dB) at null points than the wind forcing, while it did not affect high frequency (900 Hz) acoustics transmission as much as the wind forcing. The frequency spectra analysis of sound speed fluctuations and acoustic variables fluctuations in the 15-day period also verify that there is a stronger tidal signature in the transmissions of lower frequency at the deep source depth than that of the higher frequency at the shallow source depth.

The explanation is that the wind forcing usually acts more on the surface layer than the deeper layer of the water column. The tidal effects will modulate the whole water column much more efficiently than the wind forcing effects. As for sound propagation, the higher frequency sound will be scattered more than lower frequency sound inside the water column. So comparing to high frequency sound propagation, the low frequency source will generate the more clustered of sound energy in the water column, and it is modulated much more by tide than the wind forcing.

Additional study needs to be carried out to determine more quantitative measures of the acoustic prediction fluctuations due to the variations of the water column in the region. We hope to be able to obtain acoustic data to evaluate the accuracy of the acoustic predictions. We expect some discrepancies between measurements and predictions, in part due to the simplistic model of seabed bottom (a uniform half-space below the sediment layer assumptions). This simplistic model is questionable for frequencies below 10 KHz, but more certainly for frequency below 1 kHz. In addition, contribution to the mismatch might be from the rough ocean surface and also ocean water column variations and uncertainties.

ACKNOWLEDGMENTS

We thank the Office of Naval Research for supporting this research under grant PLUSNet (S05-06) and PLUS-SEAS (N00014-08-1-06 80) to MIT. We are very grateful to the whole PLUSNet team for very fruitful collaborations. In particular, we thank the crews, operators and support personnel of the ships, gliders and kayaks for their work and critical data they provided. We are grateful to Katherine H Kim and Mike Porter's team at HLSresearch for providing us with the Dabob seabed properties. We acknowledge NOAA's National Geophysical Data Center for the topography data and the Scripps Satellite Geodesy program for the larger scale topography data. We thank Tim Duda for helpful discussions.

REFERENCES

1. P. F. J. Lermusiaux. Uncertainty estimation and prediction for interdisciplinary ocean dynamics. *Journal of Computational Physics, Special issue of on "Uncertainty Quantification". J. Glimm and G. Karniadakis, Eds.*, pages 176–199, 2006.
2. P. F. J. Lermusiaux, C. S. Chiu, G. G. Gawarkiewicz, P. Abbot, A. R. Robinson, R. N. Miller, P. J. Haley, W. G. Leslie, S. J. Majumdar, A. Pang, and F. Lekien. Quantifying uncertainities in ocean predictions. *Oceanography, Special issue on "Advances in Computational Oceanography", T. Paluszkiewicz and S. Harper (Office of Naval Research), Eds.*, 19(1):92–105, 2006.
3. M. Siderius, M. Porter, P. Hursky, V. McDonald, and the KauaiEx Group. Effects of ocean thermocline variability on underwater acoustic communications. *J. Acoust. Soc. Am.*, 121(4):1895–1908, 2007.
4. A. R. Robinson and P. F. J. Lermusiaux. Prediction systems with data assimilation for coupled ocean science and ocean acoustics. In A. Tolstoy, editor, *Proceedings of the Sixth International Conference on Theoretical and Computational Acoustics*, pages 325–342. World Scientific Publishing, 2004.
5. P. F. J. Lermusiaux, P. Malanotte-Rizzoli, D. Stammer, J. Carton, J. Cummings, and A. M. Moore. Progress and prospects of u.s. data assimilation in ocean research. *Oceanography, Special issue on "Advances in Computational Oceanography", T. Paluszkiewicz and S. Harper, Eds.*, 19(1):172–183, 2006.
6. A. R. Robinson, P. F. J. Lermusiaux, and N. Q. Sloan. Data assimilation. *The Sea: The Global Coastal Ocean*, 10:541–594, 1998.
7. A. R. Robinson. Physical processes, field estimation and an approach to a interdisciplinary ocean modeling. *Earth-Science Reviews*, 40:3–54, 1996.
8. P. F. J. Lermusiaux and C. S. Chiu. Four-dimensional data assimilation for coupled physical-acoustical fields. In N.G. Pace and F.B. Jensen, editors, *Acoustic Variability*, pages 417–424. SACLANTCEN. Kluwer Academic Press, 2002.
9. P. F. J. Lermusiaux. Adaptive sampling, adaptive data assimilation and adaptive modeling. *Physica D., Special issue on "Mathematical Issues and Challenges in Data Assimilation for Geophysical Systems: Interdisciplinary Perspectives", Christopher K.R.T. Jones and Kayo Ide, Eds.*, 230:172–196, 2007.
10. O. G. Logutov and P. F. J. Lermusiaux. Inverse barotropic tidal estimation for regional ocean applications. *Ocean Modeling*, Submitted, 49pp.
11. C. M. Ferla, M. B. Porter, and F. B. Jensen. *C-SNAP: Coupled SACLANTCEN normal mode propagation loss model*. SACLANTCEN document SM-274, 1993.
12. R. A. Helton. Oceanographic and acoustic characteristics of the dabob bay range. Technical Report Interim report, 196pp., NAVAL TORPEDO STATION KEYPORT WA, 1976.
13. F. B. Jensen, W. A. Kuperman, M. B. Porter, and H. Schmidt, editors. *Computational Ocean Acoustics*. AIP series in modern acoustics and signal processing, pages 36-38. AIP Press: Springer, 2000.
14. M. B. Porter. *Personal Communication*. 2007.